PROCEEDINGS OF SCIENCE

Atmospheric monitoring by star signal analysis using a CMOS camera system for the Telescope Array Project

Marika Przybylak,[a,*] **Dorota Sobczyńska,**[b] **Kenji Shinozaki,**[c] **Michal Vrábel**[c] **and Yoshiki Tsunesada**[d,e] **on behalf of the Telescope Array Collaboration**

[a] *University of Lodz Doctoral School of Exact and Natural Sciences, 21/23 Jana Matejki Street, 90-237 Łódź, Poland*
[b] *Faculty of Physics and Applied Informatics, University of Łódź, Pomorska 149/153 Street, 90-236 Lodz, Poland*
[c] *Astrophysics Division, National Centre for Nuclear Research, Warsaw 02-093, Poland*
[d] *Graduate School of Science, Osaka Metropolitan University, 558-8585, Osaka, Japan*
[e] *Nambu Yoichiro Institute for Theoretical and Experimental Physics, Osaka Metropolitan University, 558-8585, Osaka, Japan*

E-mail: marika.przybylak@edu.uni.lodz.pl

The Telescope Array (TA) Observatory located in Utah, U.S.A., is dedicated to the study of ultra-high-energy cosmic rays (UHECRs). The project's primary aim is to investigate the energy spectrum, origin, and composition of these cosmic rays. TA employs a hybrid detection method, using surface detectors (SDs) in combination with fluorescence detectors (FDs). The observation of air showers by FDs provides more direct estimation of the energy of the primary UHECRs, which is used to calibrate the energy estimated by SDs. Atmospheric conditions play an important role in reconstructing the shower parameters. Presently, data acquired by the FDs under cloudy skies is eliminated from the scientific analysis based on the regular visual observations logged by operators in the field. In this work, we aim to additionally assess these atmospheric conditions by monitoring a part of the FD field of view with a wide-angle, high-sensitivity CMOS camera. The analysis results may be compared with the FD data to characterize the variation of the background caused by stars. In this paper, we present this CMOS camera setup and first results toward application to the UHECR observations.

39th International Cosmic Ray Conference (ICRC2025)
15–24 July 2025
Geneva, Switzerland

ICRC 2025
The Astroparticle Physics Conference
Geneva July 15-24, 2025

*Speaker

PoS(ICRC2025)364

1. Introduction

The Telescope Array (TA) project [1], encompassing its main component, the low-energy extension (TALE), and the new high-energy expansion (TA×4) operated in Utah, U.S.A., is designed to observe air showers induced by ultra-high-energy cosmic rays (UHECRs). The project utilizes fluorescence detector (FD) stations in conjunction with surface detector (SD) array, enhancing the accuracy of energy estimation and collection efficiency of showers.

For FDs, the atmosphere serves as a calorimeter (it can be considered as a 'part of the detector'). By measuring the amount of UV fluorescence light emitted at each level of the shower axis, the longitudinal profile can be determined directly, allowing the energy deposit in the atmosphere at different atmospheric depths to be determined. The total amount of energy deposited along the shower axis provides a more accurate measurement of the primary energy than that of SDs. By limiting FD operation to moonless dark nights with favorable weather conditions, FD observations play a key role in establishing the energy scale of air showers, correlating it with the energies determined by SDs using a large number of hybrid events. To further reduce the uncertainty in the energy scale, additional event selection criteria may be applied using supplementary information on atmospheric conditions.

In this paper, we present the concept of observing stars using a CMOS camera installed at the Black Rock Mesa (BRM) FD station, and our plan to utilize it primarily for assessing weather conditions. The motivation for expanding atmospheric analysis arises from the aim to improve our understanding of the energy scale discrepancy between the FD and SD, along with its associated uncertainties. The energy estimated by the SD relies on Monte Carlo simulations and is approximately 27% higher than that estimated by the FD [3]. A similar discrepancy is seen in the observed UHECR energy spectra between the Pierre Auger Observatory and the Telescope Array, where the TA energy scale is approximately 9% higher than that of Auger [2].

2. Monitoring weather conditions during TA observation

So far, LIDAR (LIght Detection And Ranging) [4] and CLF (Central Laser Facility) [5] were operated. The LIDAR system measured the extinction coefficient and the vertical aerosol optical depth (VAOD). From measurements in nights in 2007–2009, they were 0.033 km^{-1} at the ground level and 0.035 up to 5 km from the ground, respectively.

The vertical CLF laser was fired a series of shots every 30 minutes during FD observations. Located at the geometric center of all three FDs, CLF's scattered photons are observed at all three FD stations. The VAOD was determined by analyzing those signals. The average values of the all measurements prior to 2020 which is 0.04 is currently used for FD data analysis and interpretation.

We use the atmospheric profiles provided from Global Data Assimilation System (GDAS) database[6] every 3 hours in the analysis and interpretation of the data. Monitoring the cloud thickness and coverage has been primarily done visually every hour by the shifters. Based on this log, the data acquired by the FDs under cloudy skies is eliminated from the scientific analysis. However, with possible rapid changes in conditions, the goal of this work is twofold: characterizing the uncertainty in event reconstruction and filtering out events recorded under sub-optimal weather conditions.

3. Star measurements

To evaluate the atmospheric conditions at the BRM site during FD operations, we analyze the optical signals from stars captured by a dedicated CMOS camera system. Since the intensity of starlight received at ground level depends on the path that it takes through the atmosphere. In the near future, we aim at comparing these results with FD measurements. This section outlines the principle of this method and its implementation using stars as reference light sources.

3.1 Stars as "standard candles"

Due to Earth's rotation, stars appear to move across the night sky. As they change position in the sky, their brightness as seen from the ground gradually changes. This variation is mainly caused by atmospheric extinction, which occurs because starlight is weakened when passing through different amounts of Earth's atmosphere depending on the star's altitude. When a star is high in the sky, its light passes through the least amount of atmosphere, resulting in minimal signal loss and the highest observed brightness. However, as the star moves closer to the horizon, its light travels through a much longer and denser atmospheric path. This leads to more scattering and absorption, significantly reducing the detected brightness. By continuously monitoring the brightness variations of known stars throughout the night, it is possible to evaluate the influence of the atmosphere on the observed signal.

The expected stellar signal is estimated based on spectral data from the Stellar Spectral Flux Library by Pickles [7] (Hipparcos Catalogue numbers (HIP) are used to refer stars in this work). The expected light intensity in a given direction can be further refined by simulating atmospheric attenuation, assuming only Rayleigh scattering and ozone absorption, using radiative transfer codes such as LibRatran [8]. By comparing this idealized estimate with actual observations, additional information about the atmospheric conditions can be inferred. If the atmosphere remains stable over time, the signal is expected to decrease as a function of the zenith angle. Applying this method to multiple stars with different zenith angles may allow for a broader assessment of the atmospheric conditions surrounding the observation site.

3.2 CMOS camera

In March 2025, the CMOS camera system was adapted for TA use based on the DIMS (Dark matter and Interstellar Meteoroid Study) project station [9] in front of the BRM FD station. A Canon ME20F-SHN camera [10] is employed. This model is designed for extreme low-light performance, featuring a full-frame 35 mm CMOS sensor with approximately 2.26 megapixels and large 19 µm pixels. It is capable of capturing Full HD (1920 × 1080 pixels) video at 29.97 frames per second. A Canon EF 35 mm f/1.4L lens is used with a blue optical filter (300–500 nm) to limit the spectral bandwidth to approximate that of fluorescence light. The field of view (FOV) is approximately 54° × 33° pointed in the direction of azimuth ~324° and elevation ~18°.

The software for remote data acquisition and camera operation, developed for the DIMS project, has been preserved. New functions are added to regularly take 'snapshots' of the sky with variable exposure and frequency as well as the camera parameters such as the gain and f-number. In the current test configurations, we applied gains around 60 – 66 dB, which corresponds to a sensitivity of approximately ISO~800,000 – 1,600,000 out of its maximum 75 dB gain range. The aperture was

set to its maximum aperture f/1.4. In every two sidereal minutes (~119.5 s in SI units), 450 frames are integrated to produce one image with an effective exposure time of ~15 s. Each pixel contains three 8-bit RGB values representing the intensities of red, green, and blue channels, respectively. These images are used not only for monitoring the observational conditions by FD shifters in real time but also for scientific data analysis.

Each integrated image is post-processed to extract key summary data per pixel, including the sum of pixel values, standard deviation, and the peak value observed (peak-hold) across the frames. These datasets are automatically uploaded to a common server to facilitate real-time access and long-term storage. For the scientific analysis, only the blue channel values with typical sensitivity in ~380–580 nm are utilized.

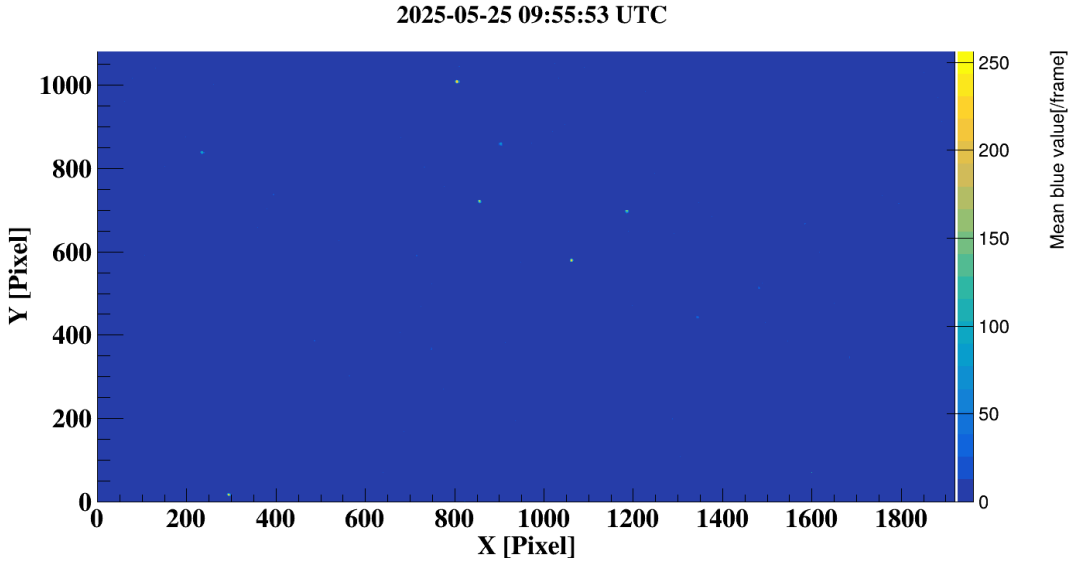

Figure 1: An example snapshot taken at May 25, 2025. The color scale indicates the mean value per frame.

In Figure 1, an example of the snapshot data obtained by the camera system on May 25, 2025, at 09:55:53 UTC is shown. The color scale indicates the mean value per frame. This time corresponds to a local sidereal time of 18h38m. The constellation Ursa Major (UMa) is visible near the center of the FOV. A light source from a ground-based surveillance camera, located at around X~290 and Y~25 in the image, is used as a fixed reference point.

The direction of pointing of each pixel was estimated using astrometric methods. The azimuth A (measured from the north toward the east) and elevation a at the four corners of the FOV are approximately as follows, starting from the lower left corner and proceeding clockwise: $(A, a) \approx (296.0°, 2.0°)$, $(291.4°, 31.1°)$, $(355.9°, 32.1°)$, $and (351°, 2.8°)$.

Figure 2 shows examples of snapshot data zoomed in on the direction of the constellation Auriga, taken under different atmospheric conditions. The left panel was taken on April 18, 2025, at 05:50:25 under good conditions and the right was on April 21, 2025, at 05:38:38 under relatively poor conditions. A clear difference in the number of recognized stars and their visible brightness is consistently observed. The corresponding local sidereal time was 12h06m in both

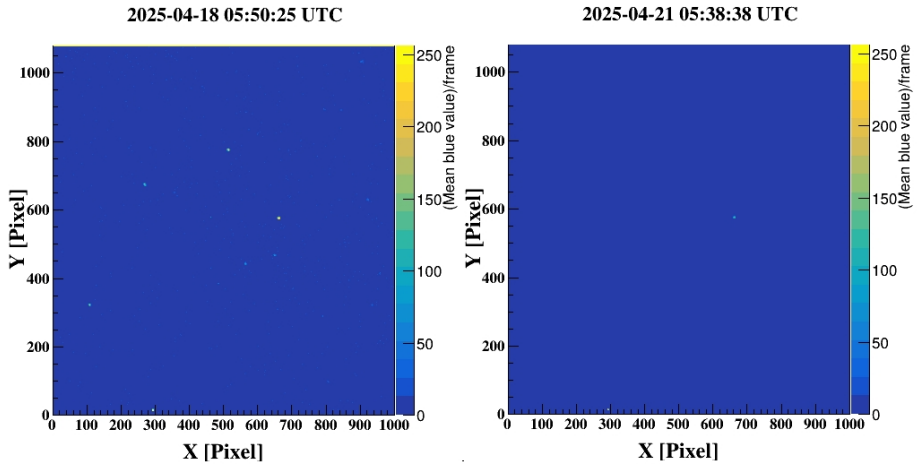

Figure 2: Examples snapshot data recorded on the same sidereal of 12h06m taken on April 18 and April 21, 2025 are shown in left and panels, respectively under different atmospheric conditions.

cases. Synchronization with sidereal time is essential, as it allows us to observe the same stars in the same positions each night. This consistency enables long-term analyses.

3.3 BRM TA FDs

The assessment of the visibility of the stars and the amount of signal reaching the FD detector [11] at the TA BRM station are also part of the visibility. It has been instrumented with 12 telescopes with a segmented 6.8-m^2 mirror each. The camera consists of 256 hexagonal photomultiplier tubes (PMTs; HAMAMATSU R9508). Each PMT pixel views approximately 1° of the sky, and the camera has a FOV of 15.5° in elevation and 18.1° in azimuth. The telescopes are installed in two-ring geometry. Six telescopes in the upper ring view from 3° to 17° in elevation. The lower ring views elevations from 17° to 31°. Both rings cover azimuths from ~240° to ~350°. The FOVs of the six northern telescopes are covered by that of the CMOS camera.

Each PMT is readout by a 10 MHz flash analog-to-digital converters (FADCs; time bin of 100 ns) with a 12-bit resolution. The system uses DC coupling, preserving both fast signals and slow baseline variations due to those night-sky background including stars. Waveforms are recorded as ADC counts over 512 time bins when the trigger conditions of the FD stations is fulfilled. The background level of each PMT may contain contributions and variability due to the passage of a star through its FOV. Bright stars can cause additional excess light across multiple PMTs as part of the night sky background. Analyzing this excess may allow us to extract further information about atmospheric conditions. In the future, modeling the comparison with CMOS output could enable the estimation of past atmospheric conditions from the FD data. The pedestal of FD PMTs are determined from the ADC counts from the data of all telescopes' PMTs that recorded at each FD trigger for air shower detection. As well as the average and standard deviation of the 8 pre-trigger time bins, the full 512-bin data are also available for reference. The trigger frequency is an order of ~Hz. Since the direction of the star is known, we can estimate the excess signal from the star by monitoring temporal variations in the pedestal along its path.

Due to a large FOV of a PMT, it also records the contributions from nearby stars and the background. Precise determination of the background which is variable over time and photometric calibration per PMT are difficult. Even bright stars do not convert to physical units easily. Since the direction of the star is known, we can estimate the excess signal from the star by monitoring temporal variations in the pedestal along its path. Using past FD data, an example of a star for HIP 62956 (ε UMa, blue band magnitude $B = +1.75$) detection by an FD telescope is shown in Figure 3. It displays the integrated pedestal levels of PMT signals, obtained from individual FD triggers and averaged over time bins, expressed in ADC counts. These values are further integrated over 6000 triggers, revealing the motion of the star in the telescope's FOV.

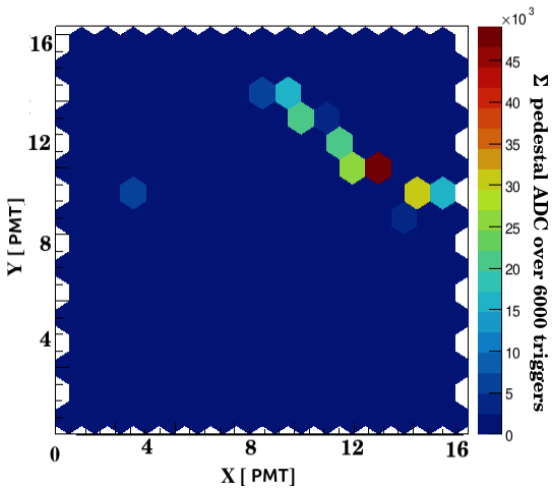

Figure 3: HIP 62956 ($B = +1.75$) detected in an FD telescope as the integrated average ADC counts of the pedestal over 6000 FD triggers, illustrating the passage of the star in an FD telescope's FOV.

4. Analysis and preliminary results from a CMOS camera system

To evaluate the feasibility of using the CMOS camera system for atmospheric monitoring, we performed a preliminary analysis of the recorded images. The primary objective was to verify whether bright stars can be detected and tracked using the current setup to seek any relative changes in brightness. We first developed algorithms that, using catalog information about the time, celestial coordinates of stars, identify which right ascension, and declination stars should be visible in the FOV under clear sky conditions. These algorithms also indicate the expected pixels where the signal from each star should appear.

In Figure 4, reconstructed tracks of bright stars are shown on the horizontal coordinates, using 57 snapshot images recorded on May 25, 2025 in the left panel. The bin size of $\sim 0.03°$ are chosen consistent with the plate scale of the CMOS pixel. The right panel compares the brightness of two stars, HIP 53910 (β UMa, $B = +2.35$) and HIP 45075 (τ UMa, $B = +5.01$), showing a difference in detected signal intensities.

Figure 5 shows the time variation of the summed signal from HIP53910 in successive bin groups along its path shown in Figure4. The horizontal axis represents time in units of 2 minutes in sidereal time. The vertical axis indicates the sum of pixel values within a 16×16 bin region defined in this study, covering the entire trajectory of the star , expressed per frame. A general decrease in signal over time is observed, corresponding to an increasing zenith angle, which is consistent with expectations.

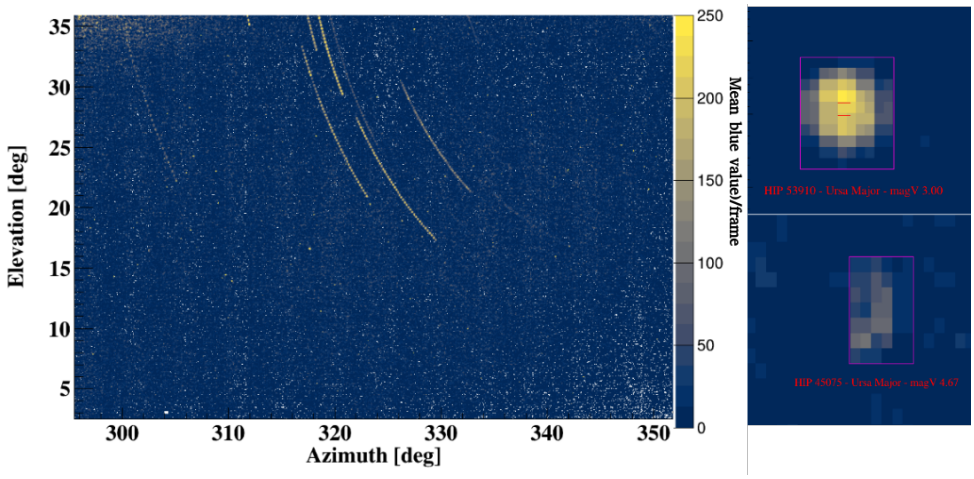

Figure 4: Left: Reconstructed star track on the horizontal coordinates as composite of 57 consecutive snapshots taken over ~117 min on May 25, 2025. Right: Comparison of stars with different brightness with HIP 53910 (B = +2.35) and HIP 45075 (B = +5.01).

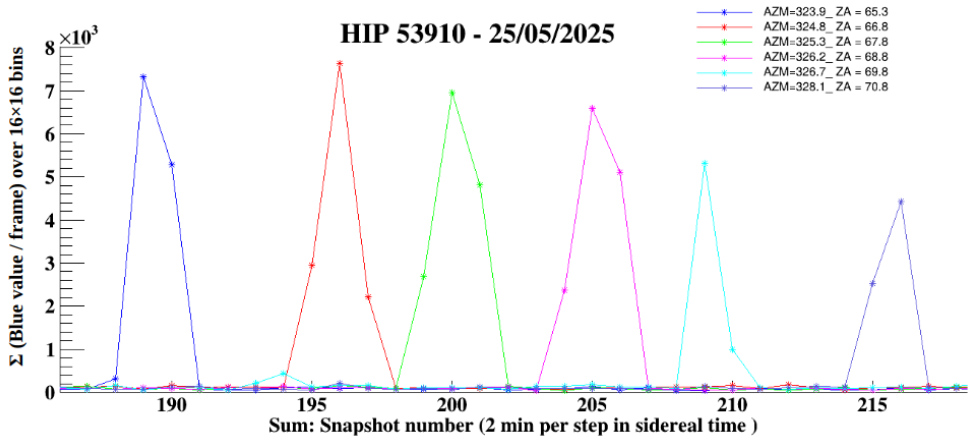

Figure 5: Signal from the star HIP 53910 as a function of time.The horizontal axis is the time in units of 2 min in sidereal time. The vertical axis denotes the sum of the values in a region of 16×16 bin as in Figure 4.

5. Summary and Outlook

In this study, we tested the feasibility of using a newly installed CMOS camera system to monitor atmospheric conditions at the BRM of the TA site. The images from the camera are also used as a quick-look monitor for FD shifters to confirm the current weather conditions. The preliminary results show that stars can be identified and tracked over time, along with their relative brightness changes. Although absolute photometric calibration with the current setup has not yet been performed, the data acquisition synchronized with sidereal time provides us with consistent measurement for stars from the catalogue. This enables relative monitoring of atmospheric conditions, which is especially useful during FD operations when the weather can change rapidly.

This system may serve as a complementary tool to existing atmospheric monitoring methods, helping to identify sub-optimal observation conditions and to support event selection during FD

data analysis. In particular, it may assist in evaluating the stability of atmospheric conditions on a time scale of minutes as well as comparison over night-to-night basis.

In the near future, we plan to compare the CMOS camera measurements with FD data to explore the possibility of using star-based modeling to review past FD data relevant to the hybrid events used for the energy scale calibration between FD and SD energies. Although still at an early stage, this work represents a first step toward developing a simple and low-maintenance method for monitoring atmospheric conditions. With further improvement, the system could provide additional information for UHECR analysis.

References

[1] J. Kim on behalf of Telescope Array Collaboration (2023), Pos(ICRC2023) 8.

[2] D.R.Bergman et al. for the Pierre Auger Collaboration and the Telescope Array Collaboration (2023), Pos(ICRC2023) 406.

[3] C.C.H. Jui for the Telescope Array Collaboration (2012), J. Phys. Conf. Ser. 404(1):012037.

[4] T. Tomida, et al. (2011), Nucl. Instrum. Meth. A654, 653.

[5] T. Tomida et al. on behalf of the Telescope Array Collaboration (2021), Pos(ICRC2021) 217.

[6] National Center for Environmental Information, NOAA, NASA, Global Data Assimilation System, https://www.ncei.noaa.gov/products/weather-climate-models/global-data-assimilation

[7] A.J. Pickles (1998), "VizieR Online Data Catalog: A Stellar Spectral Flux Library: 1150–25000 Å", originally published in Publ. Astron. Soc. Pac. 110, 863.

[8] C. Emde et al. (2016), Geosci. Model Dev. 9, 1647.

[9] S. Abe et al. for the DIMS Collaboration (2023), Pos(ICRC2023) 1376.

[10] Canon Inc., ME20F-SHN, https://global.canon/en/c-museum/product/dvc827.html

[11] H. Tokuno et al. (2012), Nucl. Instrum. Meth. A676, 54

Acknowledgement

The Telescope Array experiment is supported by the Japan Society for the Promotion of Science(JSPS) through Grants-in-Aid for Priority Area 431, for Specially Promoted Research JP21000002, for Scientific Research (S) JP19104006, for Specially Promoted Research JP15H05693, for Scientific Research (S) JP19H05607, for Scientific Research (S) JP15H05741, for Science Research (A) JP18H03705, for Young Scientists (A) JPH26707011, and for Fostering Joint International Research (B) JP19KK0074, by the joint research program of the Institute for Cosmic Ray Research (ICRR), The University of Tokyo; by the Pioneering Program of RIKEN for the Evolution of Matter in the Universe (r-EMU); by the U.S. National Science Foundation awards

PHY-1806797, PHY-2012934, PHY-2112904, PHY-2209583, PHY-2209584, and PHY-2310163, as well as AGS-1613260, AGS-1844306, and AGS-2112709; by the National Research Foundation of Korea (2017K1A4A3015188, 2020R1A2C1008230, and RS-2025-00556637) ; by the Ministry of Science and Higher Education of the Russian Federation under the contract 075-15-2024-541, IISN project No. 4.4501.18, by the Belgian Science Policy under IUAP VII/37 (ULB), by National Science Centre in Poland grant 2020/37/B/ST9/01821, by the European Union and Czech Ministry of Education, Youth and Sports through the FORTE project No. CZ.02.01.01/00/22_008/0004632, and by the Simons Foundation (00001470, NG). This work was partially supported by the grants of the joint research program of the Institute for Space-Earth Environmental Research, Nagoya University and Inter-University Research Program of the Institute for Cosmic Ray Research of University of Tokyo. The foundations of Dr. Ezekiel R. and Edna Wattis Dumke, Willard L. Eccles, and George S. and Dolores Doré Eccles all helped with generous donations. The State of Utah supported the project through its Economic Development Board, and the University of Utah through the Office of the Vice President for Research. The experimental site became available through the cooperation of the Utah School and Institutional Trust Lands Administration (SITLA), U.S. Bureau of Land Management (BLM), and the U.S. Air Force. We appreciate the assistance of the State of Utah and Fillmore offices of the BLM in crafting the Plan of Development for the site. We thank Patrick A. Shea who assisted the collaboration with much valuable advice and provided support for the collaborationâ€™s efforts. The people and the officials of Millard County, Utah have been a source of steadfast and warm support for our work which we greatly appreciate. We are indebted to the Millard County Road Department for their efforts to maintain and clear the roads which get us to our sites. We gratefully acknowledge the contribution from the technical staffs of our home institutions. An allocation of computing resources from the Center for High Performance Computing at the University of Utah as well as the Academia Sinica Grid Computing Center (ASGC) is gratefully acknowledged.
This work is supported by University of Lodz and University of Lodz Doctoral School of Exact and Natural Sciences. We gratefully acknowledge the contributions from Prof. F. Kajino, Konan University and the technical staffs of Cosmic Ray Center, University of Utah.

Telescope Array Collaboration

R.U. Abbasi[1], T. Abu-Zayyad[1,2], M. Allen[2], J.W. Belz[2], D.R. Bergman[2], F. Bradfield[3], I. Buckland[2], W. Campbell[2], B.G. Cheon[4], K. Endo[3], A. Fedynitch[5,6], T. Fujii[3,7], K. Fujisue[5,6], K. Fujita[5], M. Fukushima[5], G. Furlich[2], A. Gálvez Ureña[8], Z. Gerber[2], N. Globus[9], T. Hanaoka[10], W. Hanlon[2], N. Hayashida[11], H. He[12^{fnsymbol1}], K. Hibino[11], R. Higuchi[12], D. Ikeda[11], D. Ivanov[2], S. Jeong[13], C.C.H. Jui[2], K. Kadota[14], F. Kakimoto[11], O. Kalashev[15], K. Kasahara[16], Y. Kawachi[3], K. Kawata[5], I. Kharuk[15], E. Kido[5], H.B. Kim[4], J.H. Kim[2], J.H. Kim[2^{fnsymbol2}], S.W. Kim[13^{fnsymbol3}], R. Kobo[3], I. Komae[3], K. Komatsu[17], K. Komori[10], A. Korochkin[18], C. Koyama[5], M. Kudenko[15], M. Kuroiwa[17], Y. Kusumori[10], M. Kuznetsov[15], Y.J. Kwon[19], K.H. Lee[4], M.J. Lee[13], B. Lubsandorzhiev[15], J.P. Lundquist[2,20], H. Matsushita[3], A. Matsuzawa[17], J.A. Matthews[2], J.N. Matthews[2], K. Mizuno[17], M. Mori[10], S. Nagataki[12], K. Nakagawa[3], M. Nakahara[3], H. Nakamura[10], T. Nakamura[21], T. Nakayama[17], Y. Nakayama[10], K. Nakazawa[10], T. Nonaka[5], S. Ogio[5], H. Ohoka[5], N. Okazaki[5], M. Onishi[5],

A. Oshima[22], H. Oshima[5], S. Ozawa[23], I.H. Park[13], K.Y. Park[4], M. Potts[2], M. Przybylak[24], M.S. Pshirkov[15,25], J. Remington[2fnsymbol4], C. Rott[2], G.I. Rubtsov[15], D. Ryu[26], H. Sagawa[5], N. Sakaki[5], R. Sakamoto[10], T. Sako[5], N. Sakurai[5], S. Sakurai[3], D. Sato[17], K. Sekino[5], T. Shibata[5], J. Shikita[3], H. Shimodaira[5], H.S. Shin[3,7], K. Shinozaki[27], J.D. Smith[2], P. Sokolsky[2], B.T. Stokes[2], T.A. Stroman[2], H. Tachibana[3], K. Takahashi[5], M. Takeda[5], R. Takeishi[5], A. Taketa[28], M. Takita[5], Y. Tameda[10], K. Tanaka[29], M. Tanaka[30], M. Teramoto[10], S.B. Thomas[2], G.B. Thomson[2], P. Tinyakov[15,18], I. Tkachev[15], T. Tomida[17], S. Troitsky[15], Y. Tsunesada[3,7], S. Udo[11], F.R. Urban[8], M. Vrábel[27], D. Warren[12], K. Yamazaki[22], Y. Zhezher[5,15], Z. Zundel[2], and J. Zvirzdin[2]

[1] *Department of Physics, Loyola University-Chicago, Chicago, Illinois 60660, USA*

[2] *High Energy Astrophysics Institute and Department of Physics and Astronomy, University of Utah, Salt Lake City, Utah 84112-0830, USA*

[3] *Graduate School of Science, Osaka Metropolitan University, Sugimoto, Sumiyoshi, Osaka 558-8585, Japan*

[4] *Department of Physics and The Research Institute of Natural Science, Hanyang University, Seongdong-gu, Seoul 426-791, Korea*

[5] *Institute for Cosmic Ray Research, University of Tokyo, Kashiwa, Chiba 277-8582, Japan*

[6] *Institute of Physics, Academia Sinica, Taipei City 115201, Taiwan*

[7] *Nambu Yoichiro Institute of Theoretical and Experimental Physics, Osaka Metropolitan University, Sugimoto, Sumiyoshi, Osaka 558-8585, Japan*

[8] *CEICO, Institute of Physics, Czech Academy of Sciences, Prague 182 21, Czech Republic*

[9] *Institute of Astronomy, National Autonomous University of Mexico Ensenada Campus, Ensenada, BC 22860, Mexico*

[10] *Graduate School of Engineering, Osaka Electro-Communication University, Neyagawa-shi, Osaka 572-8530, Japan*

[11] *Faculty of Engineering, Kanagawa University, Yokohama, Kanagawa 221-8686, Japan*

[12] *Astrophysical Big Bang Laboratory, RIKEN, Wako, Saitama 351-0198, Japan*

[13] *Department of Physics, Sungkyunkwan University, Jang-an-gu, Suwon 16419, Korea*

[14] *Department of Physics, Tokyo City University, Setagaya-ku, Tokyo 158-8557, Japan*

[15] *Institute for Nuclear Research of the Russian Academy of Sciences, Moscow 117312, Russia*

[16] *Faculty of Systems Engineering and Science, Shibaura Institute of Technology, Minumaku, Tokyo 337-8570, Japan*

[17] *Academic Assembly School of Science and Technology Institute of Engineering, Shinshu University, Nagano, Nagano 380-8554, Japan*

[18] *Service de Physique Théorique, Université Libre de Bruxelles, Brussels 1050, Belgium*

[19] *Department of Physics, Yonsei University, Seodaemun-gu, Seoul 120-749, Korea*

[20] *Center for Astrophysics and Cosmology, University of Nova Gorica, Nova Gorica 5297, Slovenia*

[21] *Faculty of Science, Kochi University, Kochi, Kochi 780-8520, Japan*

[22] *College of Science and Engineering, Chubu University, Kasugai, Aichi 487-8501, Japan*

[23] *Quantum ICT Advanced Development Center, National Institute for Information and Communications Technology, Koganei, Tokyo 184-8795, Japan*

[24] *Doctoral School of Exact and Natural Sciences, University of Lodz, Lodz, Lodz 90-237, Poland*

[25] *Sternberg Astronomical Institute, Moscow M.V. Lomonosov State University, Moscow 119991, Russia*

[26] *Department of Physics, School of Natural Sciences, Ulsan National Institute of Science and Technology, UNIST-gil, Ulsan 689-798, Korea*

[27] *Astrophysics Division, National Centre for Nuclear Research, Warsaw 02-093, Poland*

[28] *Earthquake Research Institute, University of Tokyo, Bunkyo-ku, Tokyo 277-8582, Japan*

[29] *Graduate School of Information Sciences, Hiroshima City University, Hiroshima, Hiroshima 731-3194, Japan*

[30] *Institute of Particle and Nuclear Studies, KEK, Tsukuba, Ibaraki 305-0801, Japan*

^{fnsymbol1} Presently at: Purple Mountain Observatory, Nanjing 210023, China

^{fnsymbol2} Presently at: Physics Department, Brookhaven National Laboratory, Upton, NY 11973, USA

^{fnsymbol3} Presently at: Korea Institute of Geoscience and Mineral Resources, Daejeon, 34132, Korea

^{fnsymbol4} Presently at: NASA Marshall Space Flight Center, Huntsville, Alabama 35812, USA

PoS(ICRC2025)364